Coupling constant for $\Lambda(1405)\bar{K}N$

Ju-Jun Xie,[1,2,*] Bo-Chao Liu,[2,3,†] and Chun-Sheng An[4,‡]

[1]*Institute of Modern Physics, Chinese Academy of Sciences, Lanzhou 730000, China*

[2]*State Key Laboratory of Theoretical Physics, Institute of Theoretical Physics, Chinese Academy of Sciences, Beijing 100190, China*

[3]*Department of Applied Physics, Xi'an Jiaotong University, Xi'an, Shanxi 710049, China*

[4]*Institute of High Energy Physics and Theoretical Physics Center for Science Facilities, Chinese Academy of Sciences, Beijing 100049, China*

(Received 9 February 2013; revised manuscript received 11 June 2013; published 17 July 2013)

The value of the $\Lambda(1405)\bar{K}N$ coupling constant $g_{\Lambda(1405)\bar{K}N}$ is obtained by fitting it to the experimental data on the total cross sections of the $K^-p \to \pi^0\Sigma^0$ reaction. On the basis of an effective Lagrangian approach and isobar model, we show that the value $|g_{\Lambda(1405)\bar{K}N}| = 1.51 \pm 0.10$ could be extracted from the available experimental data by assuming that the s-channel $\Lambda(1405)$ resonance plays a dominant role, whereas, the background contributions from the s-channel $\Lambda(1115)$, t-channel K^*, and u-channel nucleon pole processes are small and can be neglected. However, the u-channel nucleon pole diagram may also give an important contribution in the present calculations. After the background contributions are taken into account, the above value of $g_{\Lambda(1405)\bar{K}N}$ is reduced to $|g_{\Lambda(1405)\bar{K}N}| = 0.77 \pm 0.07$, which is not supported by the previous calculations and the recent CLAS measurements. The theoretical calculations on differential cross sections are also presented, which can be checked by future experiments.

DOI: 10.1103/PhysRevC.88.015203 PACS number(s): 13.75.Jz, 13.30.Eg, 13.75.Cs, 14.20.Gk

I. INTRODUCTION

The reactions induced by a K^- meson beam are important tools for gaining a deeper understanding of the $\bar{K}N$ interaction and of the nature of the hyperon resonances. Among those reactions, the $K^-p \to \pi^0\Sigma^0$ reaction is of particular interest. Since there are no isospin-1 hyperons that contribute here, this reaction gives us a rather clean platform to study the isospin-0 Λ resonances. Furthermore, it is well known that the inelastic effects are especially important for the low-energy $\bar{K}N$ interaction because the $\bar{K}N$ channel strongly couples to the $\pi\Sigma$ channel through the $\Lambda(1405)$ resonance (spin parity $J^P = 1/2^-$). Thus, the $K^-p \to \pi^0\Sigma^0$ reaction is a good place to study the $\Lambda(1405)$ state, whose structure and properties are still controversial, even though it is catalogued as a four-star Λ resonance in the Particle Data Group (PDG) review book [1].

In the traditional quark models, $\Lambda(1405)$ is described as a p-wave q^3 baryon [2], but it can also be explained as a $\bar{K}N$ molecule [3] or a $q^4\bar{q}$ pentaquark state [4]. Besides, it was argued, within the unitary chiral theory [5–7], that two overlapping isospin $I = 0$ states are dynamically generated, and in this approach, the shape of any observed $\Lambda(1405)$ spectrum might depend upon the production process. In a recent experimental study of the $pp \to pK^+\Lambda(1405) \to pK^+(\pi\Sigma)$ reaction [8], the $\Lambda(1405)$ resonance was clearly identified through its $\pi^0\Sigma^0$ decay, and no obvious mass shift was found, which was checked in Ref. [9] by using the effective Lagrangian approach with considering only one $\Lambda(1405)$ state. However, the final answer is still absent in the sense that the experimental data could also be well described in the two-resonance scenario [10].

As shown in Refs. [11–17], the combination of the effective Lagrangian approach and the isobar model is a good method for studying the hadron resonances' production in the πN, NN, and $\bar{K}N$ scatterings. One key issue of this method is the coupling constant of the involved resonance interaction vertex, which can be obtained from the partial decay width. However, if the mass of the resonance is below the threshold of the corresponding channel, such as the $\Lambda(1405)$ ($M = 1405$ MeV) to the $\bar{K}N$ ($m_{\bar{K}} + m_N = 1434.6$ MeV) channel, it is impossible to get the coupling constant within the above procedure. For example, the strong coupling constants of the $\Lambda(1405)$ resonance were investigated within an extended chiral constituent quark model [18], whereas, in Refs. [16,19], the coupling constant of $g_{N(1535)N\phi}$ was obtained from the studies of the $\pi^-p \to n\phi$ reaction. Besides, in Ref. [20], the coupling constant of $g_{N^*(1535)N\rho}$ was studied from the analysis of the $N^*(1535) \to N\rho^0 \to N\pi^+\pi^-$ and the $N^*(1535) \to N\rho^0 \to N\gamma$ decays.

Moreover, the couplings of the $\Lambda(1405)$ resonance to the $\bar{K}N$ and $\pi\Sigma$ channels and the ratio of $g_{\Lambda(1405)\bar{K}N}$ and $g_{\Lambda(1405)\pi\Sigma}$, $R = g_{\Lambda(1405)\bar{K}N}/g_{\Lambda(1405)\pi\Sigma}$, have been intensively studied both experimentally [21] and within various theoretical approaches, for instance, the current algebra [22,23], potential models [22,24], dispersion relations [25], asymptotic SU(3) symmetry approach [26], and they were recently investigated by taking the $\Lambda(1405)$ resonance to be an admixture of traditional three-quark and higher five-quark Fock components [18]. However, the obtained values of R by different theoretical methods vary in a large range of 3.2–7.8, so it is still worth it to study the coupling constants $g_{\Lambda(1405)\bar{K}N}$ and $g_{\Lambda(1405)\pi\Sigma}$ in different ways.

In the present paper, here is one more way in this line; by using an effective Lagrangian approach and the isobar model, we extract the $\Lambda(1405)\bar{K}N$ coupling constant $g_{\Lambda(1405)\bar{K}N}$ by fitting it to the experimental data on the total cross sections of the $K^-p \to \pi^0\Sigma^0$ reaction near threshold. We also calculate

*xiejujun@impcas.ac.cn
†liubc@xjtu.edu.cn
‡ancs@ihep.ac.cn

the differential cross sections for the $K^- p \to \pi^0 \Sigma^0$ reaction with the fitted parameters. These model predictions can be checked by future experiments. For simplicity here we will work within the single $\Lambda(1405)$ state framework with parameters as reported in the PDG [1].

This article is organized as follows. In Sec. II, we present the formalism and ingredients necessary for our calculations. In Sec. III, we present the values of the obtained coupling constants. The theoretical calculations on the differential cross sections are also shown. A short summary is given in the last section.

II. FORMALISM AND INGREDIENTS

The combination of the isobar model and the effective Lagrangian method is a useful theoretical approach in the description of various processes in the resonance production region. In this section, we introduce the theoretical formalism and ingredients for calculating the cross sections of the $K^- p \to \pi^0 \Sigma^0$ reaction within the effective Lagrangian method.

The basic tree-level Feynman diagrams for the $K^- p \to \pi^0 \Sigma^0$ reaction are shown in Fig. 1. These include the t-channel K^* exchange [Fig. 1(a)], the u-channel proton exchange [Fig. 1(b)], and the s-channel $\Lambda(1115)$ and $\Lambda(1405)(\equiv \Lambda^*)$ processes [Fig. 1(c)]. To compute the contributions of these terms, we use the effective interaction Lagrangian densities as used in Refs. [27–31],

$$\mathcal{L}_{K^* K\pi} = -g_{K^* K\pi}(\vec{\pi}\cdot\tau\,\partial^\mu \bar{K} - \bar{K}\,\partial^\mu \vec{\pi}\cdot\tau) K^*_\mu, \tag{1}$$

$$\mathcal{L}_{K^* N\Sigma} = -i g_{K^* N\Sigma} \bar{N}\left(\gamma_\mu - \frac{\kappa}{2M_N}\sigma_{\mu\nu}\partial^\nu\right) K^{*\mu}\vec{\Sigma}\cdot\tau + \text{H.c.}, \tag{2}$$

for the t-channel K^* exchange, and

$$\mathcal{L}_{\pi NN} = -i g_{\pi NN}\bar{N}\gamma_5\vec{\pi}\cdot\tau N + \text{H.c.}, \tag{3}$$

$$\mathcal{L}_{KN\Sigma} = -i g_{KN\Sigma}\bar{N}\gamma_5\vec{\Sigma}\cdot\tau K + \text{H.c.}, \tag{4}$$

$$\mathcal{L}_{KN\Lambda} = -i g_{KN\Lambda}\bar{N}\gamma_5\Lambda K + \text{H.c.}, \tag{5}$$

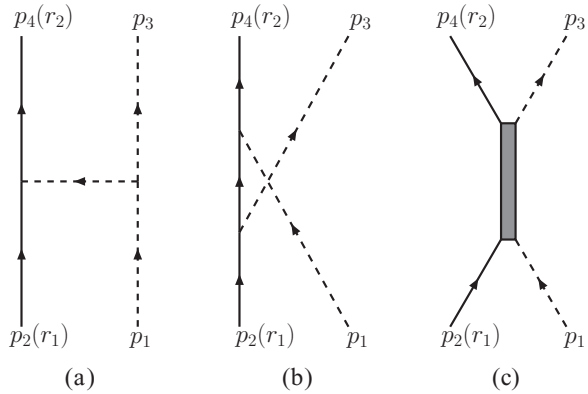

FIG. 1. Feynman diagrams for the reaction $K^- p \to \pi^0 \Sigma^0$. In these diagrams, we show the definitions of the kinematical (p_1, p_2, p_3, p_4) and polarization variables r_1, r_2 that we use in our calculation.

for the u-channel proton pole diagram, whereas,

$$\mathcal{L}_{\pi\Sigma\Lambda} = -i g_{\pi\Sigma\Lambda}\bar{N}\gamma_5\Lambda\vec{\pi}\cdot\vec{\Sigma} + \text{H.c.}, \tag{6}$$

$$\mathcal{L}_{\Lambda^* \bar{K} N} = -i g_{\Lambda^* \bar{K} N}\bar{\Lambda}^*\bar{K}N + \text{H.c.}, \tag{7}$$

$$\mathcal{L}_{\Lambda^*\pi\Sigma} = -i g_{\Lambda^*\pi\Sigma}\bar{\Lambda}^*\vec{\pi}\cdot\vec{\Sigma} + \text{H.c.}, \tag{8}$$

for the s-channel $\Lambda(1115)$ and $\Lambda(1405)$ terms.

For the coupling constants in the above Lagrangian densities, we take $g_{\pi NN} = 13.45$ (obtained with $g^2_{\pi NN}/4\pi = 14.4$), $g_{KN\Lambda} = -13.98$, $g_{\pi\Sigma\Lambda} = 9.32$, and $g_{KN\Sigma} = 2.69$ as that determined within the SU(3) flavor symmetry [32].[1] For the $K^* N\Sigma$ couplings, we take $g_{K^* N\Sigma} = -2.36$ and $\kappa = -0.47$ as used in Ref. [33] for the calculation of the $K^*\Lambda$ photoproduction, whereas, the coupling constants $g_{K^* K\pi}$ and $g_{\Lambda^*\pi\Sigma}$ are determined from the experimentally observed partial decay widths of $K^* \to K\pi$ and $\Lambda(1405) \to \pi\Sigma$, respectively,

$$\Gamma_{K^* \to K\pi} = \frac{g^2_{K^* K\pi}}{2\pi}\frac{|\vec{p}_\pi^{\,\text{c.m.}}|^3}{m^2_{K^*}}, \tag{9}$$

$$\Gamma_{\Lambda^* \to \pi\Sigma} = \frac{3 g^2_{\Lambda^*\pi\Sigma}}{4\pi}(E_\Sigma + m_\Sigma)\frac{|\vec{p}_\Sigma|}{M_{\Lambda^*}}, \tag{10}$$

where

$$|\vec{p}_\pi^{\,\text{c.m.}}| = \frac{\sqrt{[m^2_{K^*} - (m_K + m_\pi)^2][m^2_{K^*} - (m_K - m_\pi)^2]}}{2m_{K^*}},$$

$$E_\Sigma = \frac{M^2_{\Lambda^*} + m^2_\Sigma - m^2_\pi}{2M_{\Lambda^*}},$$

$$|\vec{p}_\Sigma| = \sqrt{E^2_\Sigma - m^2_\Sigma}.$$

With masses ($m_{K^*} = 893.1$, $m_K = 495.6$, $m_\pi = 138.04$, and $M_{\Lambda^*} = 1405.1^{+1.3}_{-1.0}$ MeV), total decay widths ($\Gamma_{K^*} = 49.3$ and $\Gamma_{\Lambda^*} = 50 \pm 2$ MeV), and the decay branching ratio of $K^* \to K\pi$ and $\Lambda(1405) \to \pi\Sigma$ [$\text{Br}(K^* \to K\pi) \sim 1$ and $\text{Br}(\Lambda(1405) \to \pi\Sigma) \sim 1$], we obtain $g_{K^* K\pi} = 3.25$ and $|g_{\Lambda^*\pi\Sigma}| = 0.90 \pm 0.02$ by considering the uncertainties of the total decay width and the mass of the $\Lambda(1405)$ resonance.

With the effective Lagrangian densities given above, we can easily construct the invariant scattering amplitude,

$$\mathcal{M}_i = \bar{u}_{r_2}(p_4)\mathcal{A}_i u_{r_1}(p_2), \tag{11}$$

where i denotes the s-, t-, or u-channel process and $\bar{u}_{r_2}(p_4)$ and $u_{r_1}(p_2)$ are the spinors of the outgoing Σ^0 baryon and the initial proton, respectively. The reduced $\mathcal{A}_i$'s read

$$\mathcal{A}_s^{\Lambda(1115)} = -i g_{KN\Lambda} g_{\pi\Sigma\Lambda}\frac{\not{p}_1 + \not{p}_2 - m_\Lambda}{s - m^2_\Lambda}, \tag{12}$$

$$\mathcal{A}_s^{\Lambda(1405)} = i g_{\Lambda^* \bar{K} N} g_{\Lambda^*\pi\Sigma}\frac{\not{p}_1 + \not{p}_2 + M_{\Lambda^*}}{s - M^2_{\Lambda^*} + i M_{\Lambda^*}\Gamma_{\Lambda^*}}, \tag{13}$$

[1] Here we show the relations of these coupling constants in terms of $g_{\pi NN}$ and $\alpha = 0.4$: $g_{KN\Lambda} = -\frac{g_{\pi NN}}{\sqrt{3}}(1 + 2\alpha)$, $g_{KN\Sigma} = g_{\pi NN}(1 - 2\alpha)$, and $g_{\pi\Sigma\Lambda} = \frac{2 g_{\pi NN}}{\sqrt{3}}(1 - \alpha)$.

$$\mathcal{A}_t = -\frac{g_{K^*K\pi}g_{K^*\Sigma N}}{q^2 - m_{K^*}^2}\left(\not{p}_1 + \not{p}_3 - \frac{m_K^2 - m_\pi^2}{m_{K^*}^2}\not{q} - \frac{\kappa}{m_N}(\not{p}_1 \cdot p_3 - \not{p}_1 \not{p}_3)\right), \quad (14)$$

$$\mathcal{A}_u = g_{K\Sigma N}g_{\pi NN}\frac{\not{p}_2 - \not{p}_3 - m_N}{u - m_N^2}. \quad (15)$$

where q is the momentum of exchanged meson K^* in the t channel, whereas, $s = (p_1 + p_2)^2$ is the invariant mass square of the $K^- p$ system. As we can see, in the tree-level approximation, only the products, such as $g_{\Lambda^*\bar{K}N}g_{\Lambda^*\pi\Sigma}$ enter in the invariant amplitudes. They are determined by fitting them to the low-energy experimental data on the total cross sections of the $K^- p \to \pi^0\Sigma^0$ reaction [34] with the usage of the MINUIT fitting program. Besides, M_{Λ^*} and Γ_{Λ^*} are the mass and total decay width of the $\Lambda(1405)$ resonance for which we will take the average values as quoted in the PDG [1].

As we are not dealing with pointlike particles, we should introduce the compositeness of the hadrons. This is usually achieved by including form factors in the finite interaction vertexes. In the present paper, we adopt the following form factors [27,29,30,35]:

$$F(q_{ex}^2, M_{ex}) = \frac{\Lambda^4}{\Lambda^4 + (q_{ex}^2 - M_{ex}^2)^2} \quad (16)$$

for all channels where the q_{ex} and M_{ex} are the four-momenta and the mass of the exchanged hadron, respectively. In the present calculation, the cutoff parameter Λ is constrained between 0.6 and 1.2 GeV for all channels.

III. NUMERICAL RESULTS AND DISCUSSION

The differential cross section for $K^- p \to \pi^0\Sigma^0$ at the center of mass (c.m.) frame can be expressed as

$$\frac{d\sigma}{d\cos\theta} = \frac{1}{32\pi s}\frac{|\vec{p}_3^{\,\text{c.m.}}|}{|\vec{p}_1^{\,\text{c.m.}}|}\left(\frac{1}{2}\sum_{r_1,r_2}|\mathcal{M}|^2\right), \quad (17)$$

where θ denotes the angle of the outgoing π^0 relative to the beam direction in the c.m. frame, $\vec{p}_1$ and $\vec{p}_3$ are the three-momenta of the initial K^- and the final π^0 mesons, respectively, whereas, the total invariant scattering amplitude $\mathcal{M}$ is given by[2]

$$\mathcal{M} = \mathcal{M}_s + \mathcal{M}_t + \mathcal{M}_u. \quad (18)$$

First, by including all the contributions from the s-channel $\Lambda(1405)$ resonance, s-channel $\Lambda(1115)$, t-channel K^*, and u-channel proton processes, at a fixed cutoff parameter Λ, we perform a χ^2 fit (Fit I) to the total cross-sectional data taken from Ref. [34]. It is worth noting that since we want to get the coupling constant $g_{\Lambda(1405)\bar{K}N}$ from the total cross sections of the $K^- p \to \pi^0\Sigma^0$ reaction, the contributions from other Λ resonance are neglected. In the present paper, only the experimental data very close to the reaction threshold are taken into account, whereas, those data below the production threshold of $\Lambda(1520)$, which is the next Λ resonance above $\Lambda(1405)$, are neglected. Then there are totally ten available data points.

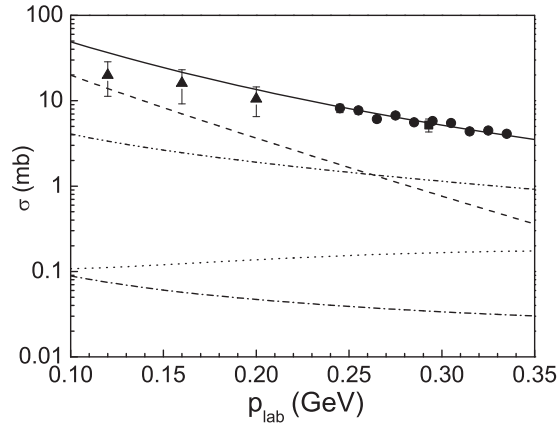

FIG. 2. The $K^- p \to \pi^0\Sigma^0$ total cross sections compared with the experimental data from Ref. [34] (dots), Ref. [36] (triangles), and Ref. [37] (squares). The results have been obtained from Fit I. The solid line represents the full results, whereas, the contribution from the s-channel $\Lambda(1405)$ resonance, s-channel $\Lambda(1115)$, t-channel K^*, and u-channel proton processes are shown by the dashed, dotted, dot-dashed, and dot-dot-dashed lines, respectively.

By constraining the value of the cutoff parameter Λ from 0.6 to 1.2 GeV, we get the minimal $\chi^2/dof = 0.9$ with $\Lambda = 0.6$ GeV for all the channels, and the fitted parameter $g_{\Lambda^*\bar{K}N}g_{\Lambda^*\pi\Sigma}$ is -0.70 ± 0.06. From the value of $g_{\Lambda^*\pi\Sigma}$, we can get $|g_{\Lambda^*\bar{K}N}| = 0.77 \pm 0.07$.

The corresponding best-fitting results of Fit I for the total cross sections are shown in Fig. 2, which compare with the experimental data. We also show, in Fig. 2, the experimental data with larger errors from Ref. [36] and one data point from Ref. [37] for comparison. The solid line represents the full results, whereas, the contributions from the s-channel $\Lambda(1405)$ resonance, s-channel $\Lambda(1115)$, t-, and u-channel diagrams are shown by dashed, dotted, and dot-dashed lines, respectively. From Fig. 2, one can see that we could describe the near-threshold data of the $K^- p \to \pi^0\Sigma^0$ reaction quite well, and the s-channel $\Lambda(1405)$ resonance and u-channel proton pole give the dominant contributions, whereas, the s-channel $\Lambda(1115)$ process and t-channel K^* exchange give minor contributions. Theoretically, it is important to find some observables to distinguish the relative roles of individual mechanisms. In Fig. 3, the corresponding theoretical calculation results for the differential cross sections at $p_{\text{lab}} = 0.15$ GeV [Fig. 3(a)], $p_{\text{lab}} = 0.25$ GeV [Fig. 3(b)], and $p_{\text{lab}} = 0.35$ GeV [Fig. 3(c)] are shown, which can be tested by future experiments.

For the role of the u-channel proton pole diagram, since there could be large SU(3) flavor symmetry violation, as

[2]In phenomenological Lagrangian approaches, the relative phases between different amplitudes are not fixed. In general, we should introduce a relative phase between different amplitudes as a free parameter since now we have only few experimental data on the total cross sections, which are not sensitive to the relative phases, so we take all the relative phases as zero.

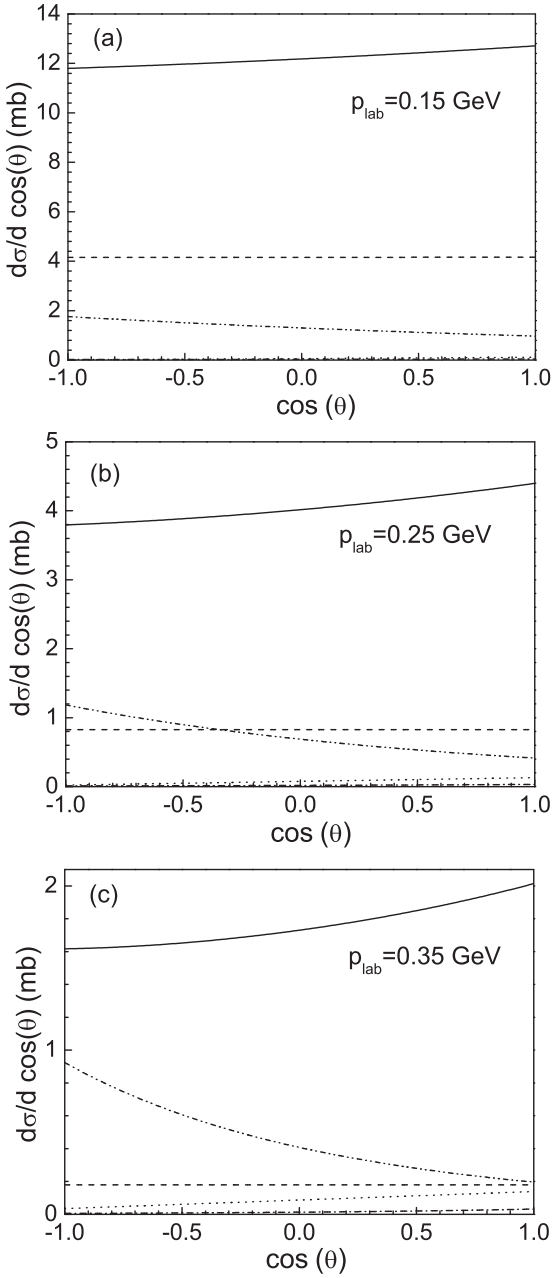

FIG. 3. The $K^- p \to \pi^0 \Sigma^0$ differential cross sections at different energies. Results have been obtained from Fit I. The solid line represents the full results, whereas, the contribution from the s-channel $\Lambda(1405)$ resonance, s-channel $\Lambda(1115)$, t-channel K^*, and u-channel proton processes are shown by the dashed, dotted, dot-dashed, and dot-dot-dashed lines, respectively.

summarized in Ref. [38] (see Table II of this reference), the value of $g_{KN\Sigma}$ lies in a very wide range. Besides, the contributions from the s-channel $\Lambda(1115)$ and t-channel diagrams are very small, so, next, we try the fit with considering the contribution from only the s-channel $\Lambda(1405)$ resonance (Fit II). In this case, we have two free parameters, which are $g_{\Lambda^*\bar{K}N} g_{\Lambda^*\pi\Sigma}$ and the cutoff parameter $\Lambda_s^{\Lambda(1405)}$. The fitted results are $g_{\Lambda^*\bar{K}N} g_{\Lambda^*\pi\Sigma} = 1.36 \pm 0.08$, which gives $|g_{\Lambda^*\bar{K}N}| = 1.51 \pm 0.10$ and $\Lambda_s^{\Lambda(1405)} = 3.00 \pm 2.62$ GeV with

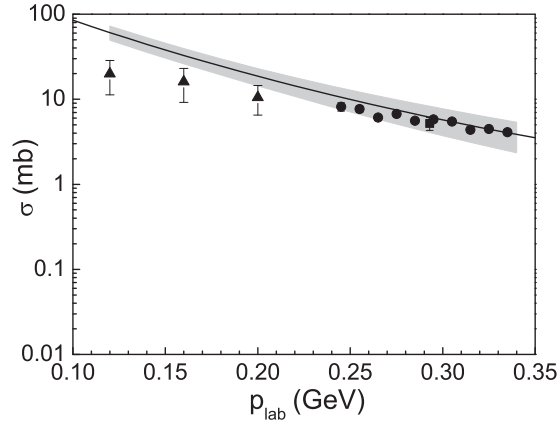

FIG. 4. As in Fig. 2 but for the best-fitted results of Fit II. We also show the error band, which is obtained from the uncertainties of the fitted parameters.

a large $\chi^2/dof = 1.7$. The corresponding results for the total cross sections are shown in Fig. 4 with the solid line. We also show the 90% confidence-level band obtained from the statistical uncertainties of the fitted parameters.[3] The results show that we can also give a reasonable description for the experimental data by only including the s-channel $\Lambda(1405)$ resonance. However, even by considering the errors of the theoretical calculation, we still cannot give a reasonable description for the data points from Ref. [36].

The value of $|g_{\Lambda^*\bar{K}N}| = 1.51 \pm 0.10$ is comparable with the value 1.84 [9], which was obtained from the separable potential model [39]. In contrast to the unitary chiral theory [6], the separable model produces only a single $\Lambda(1405)$ pole, and this is consistent with our assumption that we only include one $\Lambda(1405)$ state in the present calculation for simplicity.

From the fitted parameters of Fit II, we find an unrealistic central value of 3.00 GeV for the cutoff $\Lambda_s^{\Lambda(1405)}$ parameter with a large error (2.62 GeV), which indicates that χ^2 is rather insensitive to this parameter, so, next we fix the cutoff at some values, then only fit the one parameter $g_{\Lambda^*\bar{K}N} g_{\Lambda^*\pi\Sigma}$ to the total cross-sectional data, from which we can get the fitted coupling constant $g_{\Lambda^*\bar{K}N}$ as a function of the cutoff parameter $\Lambda_s^{\Lambda(1405)}$. The results are shown in Fig. 5. We can see from the figure that the value of $|g_{\Lambda^*\bar{K}N}|$ is stable at 1.5 within a very wide range of the cutoff parameter $\Lambda_s^{\Lambda(1405)}$.

From the values $|g_{\Lambda(1405)\bar{K}N}| = 1.51 \pm 0.10$ and $|g_{\Lambda^*\pi\Sigma}| = 0.90 \pm 0.02$, we can easily obtain the ratio $R = |g_{\Lambda^*\bar{K}N}/g_{\Lambda^*\pi\Sigma}| = 1.68 \pm 0.12$,[4] which is smaller than those obtained from different models: 2.19 obtained by using an algebra-of-currents approach [22] and 2.61 ± 1.34 extracted

[3] We generate pairs of parameters ($g_{\Lambda^*\bar{K}N} g_{\Lambda^*\pi\Sigma}$ and $\Lambda_s^{\Lambda(1405)}$) from a two-dimensional correlated Gaussian distribution with the mean values and standard deviations obtained from the best χ^2 fit. For each ($g_{\Lambda^*\bar{K}N} g_{\Lambda^*\pi\Sigma}$ and $\Lambda_s^{\Lambda(1405)}$) pair, we calculate the total cross sections. We plot all these results and throw away the upper 5% and the lower 5%, then the band, shown in Fig. 4, is obtained.

[4] If we take the values of 0.77 from Fit I and 1.51 from Fit II as the lower and upper limits, respectively, for $g_{\Lambda^*\bar{K}N}$, we then can get $|g_{\Lambda^*\bar{K}N}| = 1.14 \pm 0.37$, which gives $R = 1.27 \pm 0.41$.

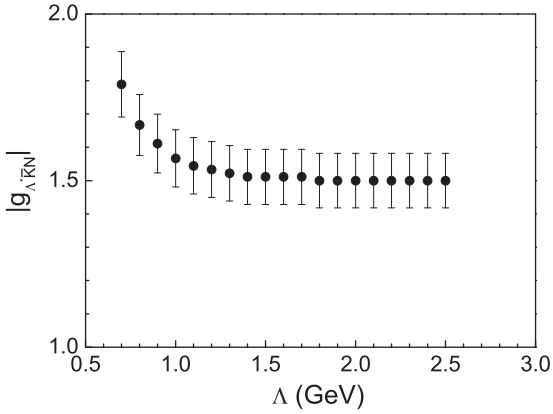

FIG. 5. Coupling constant $|g_{\Lambda^*\bar{K}N}|$ versus the cutoff parameter Λ.

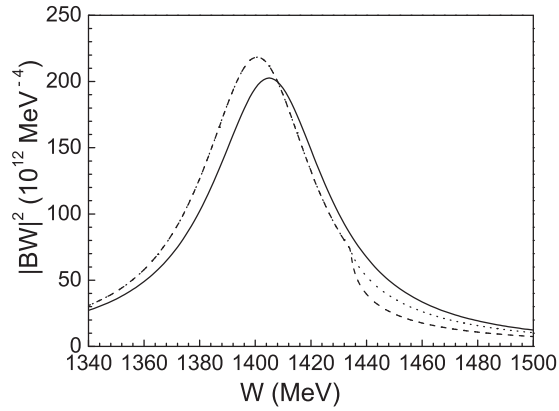

FIG. 6. The module square of the Breit-Wigner function for $\Lambda^*(1405)$ versus W with a constant total decay width (solid line) and an energy-dependent width with the form in Eq. (20) with $g_{\Lambda^*\bar{K}N} = 1.51$ (dashed line) and $g_{\Lambda^*\bar{K}N} = 0.77$ (dotted line).

from the coupled-channel analysis of the $K^- p$ scattering [40]. We show these values and the couplings of $\Lambda^*\bar{K}N$ and $\Lambda^*\pi\Sigma$ in Table I for comparison. From Table I, we find that even the values of R are different, but the values for $|g_{\Lambda^*\bar{K}N}|$ are similar within the errors.

On the other hand, in analysis of the line shapes of the $\Sigma\pi$ final states in the production reaction $\gamma p \to K^+ + (\Sigma\pi)$, it is convenient to parametrize the scattering amplitude in the isospin-0 sector as the Breit-Wigner function BW(W), which has been used in Ref. [41],

$$\mathrm{BW}(W) = \frac{1}{W^2 - M^2_{\Lambda^*} + iM_{\Lambda^*}\Gamma_{\Lambda^*}(W)}, \tag{19}$$

where W is the invariant mass of the $\Sigma\pi$ system and $\Gamma_{\Lambda^*}(W)$ is the energy-dependent width that accounts for all the decay channels; this is because in the $\gamma p \to K^+ + (\Sigma\pi)$ reaction, the $N\bar{K}$ channel opens within the range of the mass distribution of the $\Sigma\pi$ system.

By considering the $\Lambda^*(1405)\bar{K}N$ coupling by using the Flatté prescription [42], the energy-dependent total decay width for the $\Lambda^*(1405)$ resonance, is[5]

$$\Gamma_{\Lambda^*}(W) = \frac{3g^2_{\Lambda^*\pi\Sigma}}{4\pi}[E_\Sigma + m_\Sigma]\frac{|\vec{p}_\Sigma|}{W} + \frac{g^2_{\Lambda^*\bar{K}N}}{2\pi}[E_N + m_N]\frac{|\vec{p}_N|}{W}\theta(W - m_{\bar{K}} - m_N), \tag{20}$$

with

$$E_{\Sigma/N} = \frac{W^2 + m^2_{\Sigma/N} - m^2_{\pi/\bar{K}}}{2W}, \tag{21}$$

$$|\vec{p_{\Sigma/N}}| = \sqrt{E^2_{\Sigma/N} - m^2_{\Sigma/N}}. \tag{22}$$

In Fig. 6, we show the results for the module square of BW(W) as a function of W. The solid line stands for the results obtained with a constant total decay width (50 MeV), whereas, the dashed and dotted lines are obtained with $g_{\Lambda^*\bar{K}N} = 1.51$ and $g_{\Lambda^*\bar{K}N} = 0.77$, respectively, by using the energy-dependent width with the form in Eq. (20). From the results, we find that the Breit-Wigner mass will be pushed down if we use the energy-dependent width, and there is a clear drop in the module-squared distribution at the $\bar{K}N$ threshold with a larger value of $g_{\Lambda(1405)\bar{K}N} = 1.51$. However, the smaller value of $g_{\Lambda(1405)\bar{K}N} = 0.77$ could not give a clear drop for the module-squared distribution at the $\bar{K}N$ threshold. The very recent experimental results measured by the CLAS Collaboration in Ref. [41] show that there is a sharp drop in the $\Sigma\pi$ mass distributions, and this could be reproduced by using the above BW(W) formalism with the large coupling constant $g_{\Lambda(1405)\bar{K}N}$.

[5]We mention that, in the present calculation since the $\bar{K}N$ channel is opened, we just use a constant total decay width for the $\Lambda(1405)$ resonance in such a way that we can also reduce the number of free parameters. Furthermore, we do not continue the decay momentum to imaginary values, which means below the threshold of the decay channel, we take the decay momentum as zero.

TABLE I. Couplings of $\Lambda(1405)\bar{K}N$ and $\Lambda(1405)\pi\Sigma$.

$\lvert g_{\Lambda^*\bar{K}N}\rvert$	$\lvert g_{\Lambda^*\pi\Sigma}\rvert$	R	Reference
1.64	0.75	2.19	[22]
2.10 ± 0.71	0.77 ± 0.30	2.61 ± 1.34	[40]
1.51 ± 0.10	0.90 ± 0.02	1.68 ± 0.12	This paper

IV. SUMMARY

In this paper, the value of the $\Lambda(1405)\bar{K}N$ coupling constant $g_{\Lambda(1405)\bar{K}N}$ is obtained by fitting it to the low-energy experimental data of the $K^- p \to \pi^0\Sigma^0$ reaction. On the basis of an effective Lagrangian approach, we show that the value of the $\Lambda(1405)\bar{K}N$ coupling constant $|g_{\Lambda(1405)\bar{K}N}| = 0.77 \pm 0.07$ can be extracted from the available low-energy experimental data of the total cross section of the $K^- p \to \pi^0\Sigma^0$ reaction by including the s-channel $\Lambda(1405)$ resonance, s-channel $\Lambda(1115)$ process, t-channel K^*, and u-channel proton pole diagrams. On the other hand, by including only the contribution from the s-channel $\Lambda(1405)$ resonance, we get $|g_{\Lambda(1405)\bar{K}N}| = 1.51 \pm 0.10$, which is supported by the previous calculations [22,40] as shown in Table I.

Due to the violation of the SU(3) flavor symmetry, the contribution from the u channel could be small, and we show that the differential cross sections shown in Fig. 3 could help us to clarify whether the u-channel contribution is important or not.

We also calculate the module square of the Briet-Wigner function for the $\Lambda(1405)$ resonance with an energy-dependent total decay width with the form as the Flatté prescription [42]. The results show that the Breit-Wigner mass of the $\Lambda(1405)$ resonance will be pushed down, and there is a clear drop in the module-squared distribution at the $\bar{K}N$ threshold if we take a larger value $g_{\Lambda(1405)\bar{K}N} = 1.51$. The clear drop could explain the sharp drop that was found in the $\Sigma\pi$ mass distribution in the recent experimental measurements [41] by the CLAS Collaboration.

Finally, we would like to stress that the coupling constant $g_{\Lambda(1405)\bar{K}N}$ is important for studying the $\Lambda(1405)$ resonance in the $\gamma p \to K^+\Lambda(1405) \to K^+(\pi\Sigma)$ reaction and in the $pp \to pK^+\Lambda(1405) \to pK^+(\pi\Sigma)$ reaction by using the effective Lagrangian approach [9,43,44]. More and accurate data for these reactions can be used to improve our knowledge on the structure and properties of the $\Lambda(1405)$ state, which are, at present, still controversial.

ACKNOWLEDGMENTS

We would like to thank X.-H. Zhong, J. He, and X. Cao for useful discussions. This work was partly supported by the National Natural Science Foundation of China under Grants No. 11105126, No. 10905046, and No. 11205164.

[1] J. Beringer *et al.* (Particle Data Group), Phys. Rev. D **86**, 010001 (2012).
[2] N. Isgur and G. Karl, Phys. Rev. D **18**, 4187 (1978).
[3] R. H. Dalitz and S. F. Tuan, Ann. Phys. (NY) **10**, 307 (1960).
[4] T. Inoue, Nucl. Phys. A **790**, 530 (2007).
[5] N. Kaiser, T. Waas, and W. Weise, Nucl. Phys. A **612**, 297 (1997).
[6] E. Oset and A. Ramos, Nucl. Phys. A **635**, 99 (1998); E. Oset, A. Ramos, and C. Bennhold, Phys. Lett. B **527**, 99 (2002); J. A. Oller and U.-G. Meißner, *ibid.* **500**, 263 (2001); D. Jido, J. A. Oller, E. Oset, and U.-G. Meißner, Nucl. Phys. A **725**, 181 (2003); C. García-Recio, J. Nieves, E. R. Arriola, and M. J. V. Vacas, Phys. Rev. D **67**, 076009 (2003); T. Hyodo, S. I. Nam, D. Jido, and A. Hosaka, Phys. Rev. C **68**, 018201 (2003).
[7] C. García-Recio, M. F. M. Lutz, and J. Nieves, Phys. Lett. B **582**, 49 (2004).
[8] I. Zychor *et al.*, Phys. Lett. B **660**, 167 (2008).
[9] J.-J. Xie and C. Wilkin, Phys. Rev. C **82**, 025210 (2010).
[10] L. S. Geng and E. Oset, Eur. Phys. J. A **34**, 405 (2007).
[11] K. Tsushima, A. Sibirtsev, and A. W. Thomas, Phys. Rev. C **62**, 064904 (2000).
[12] A. Sibirtsev, J. Haidenbauer, H.-W. Hammer, and S. Krewald, Eur. Phys. J. A **27**, 269 (2006).
[13] R. Shyam, Phys. Rev. C **60**, 055213 (1999).
[14] B. C. Liu and B. S. Zou, Phys. Rev. Lett. **96**, 042002 (2006); **98**, 039102 (2007); Commun. Theor. Phys. **46**, 501 (2006).
[15] J.-J. Xie and B.-S. Zou, Phys. Lett. B **649**, 405 (2007); J.-J. Xie, B.-S. Zou, and B.-C. Liu, Chin. Phys. Lett. **22**, 2215 (2005).
[16] J.-J. Xie, B.-S. Zou, and H.-C. Chiang, Phys. Rev. C **77**, 015206 (2008).
[17] P. Gao, B. S. Zou, and A. Sibirtsev, Nucl. Phys. A **867**, 41 (2011); P. Gao, J. Shi, and B. S. Zou, Phys. Rev. C **86**, 025201 (2012).
[18] C. S. An, B. Saghai, S. G. Yuan, and J. He, Phys. Rev. C **81**, 045203 (2010).
[19] J.-P. Dai, P.-N. Shen, J.-J. Xie, and B.-S. Zou, Phys. Rev. D **85**, 014011 (2012).
[20] J.-J. Xie, C. Wilkin, and B.-S. Zou, Phys. Rev. C **77**, 058202 (2008).
[21] R. D. Tripp *et al.*, Phys. Rev. Lett. **21**, 1721 (1968); O. Braun *et al.*, Nucl. Phys. B **129**, 1 (1977).
[22] C. Weil, Phys. Rev. **161**, 1682 (1967).
[23] M. Gell-Mann, R. J. Ookes, and B. Renner, Phys. Rev. **175**, 2195 (1968).
[24] R. H. Dalitz, T. C. Wong, and G. Rajasekaran, Phys. Rev. **153**, 1617 (1967).
[25] A. D. Martin, Phys. Lett. B **65**, 346 (1976).
[26] S. Oneda and S. Matsuda, Phys. Rev. D **2**, 887 (1970).
[27] F. Q. Wu, B. S. Zou, L. Li, and D. V. Bugg, Nucl. Phys. A **735**, 111 (2004); F. Q. Wu and B. S. Zou, Phys. Rev. D **73**, 114008 (2006).
[28] B.-S. Zou and J.-J. Xie, Int. J. Mod. Phys. E **17**, 1753 (2008).
[29] G. Penner and U. Mosel, Phys. Rev. C **66**, 055211 (2002); **66**, 055212 (2002); V. Shklyar, H. Lenske, and U. Mosel, *ibid.* **72**, 015210 (2005).
[30] T. Feuster and U. Mosel, Phys. Rev. C **58**, 457 (1998); **59**, 460 (1999).
[31] M. Döring, C. Hanhart, F. Huang, S. Krewald, U.-G. Meissner, and D. Ronchen, Nucl. Phys. A **851**, 58 (2011).
[32] J. J. Swart, Rev. Mod. Phys. **35**, 916 (1963); **37**, 326 (1965).
[33] S.-H. Kim, S.-i. Nam, Y. Oh, and H.-C. Kim, Phys. Rev. D **84**, 114023 (2011).
[34] T. S. Mast *et al.*, Phys. Rev. D **11**, 3078 (1975).
[35] Y. Oh and H. Kim, Phys. Rev. C **73**, 065202 (2006); Y. Oh, K. Nakayama, and T. S. H. Lee, Phys. Rep. **423**, 49 (2006); Y. Oh, C. M. Ko, and K. Nakayama, Phys. Rev. C **77**, 045204 (2008).
[36] J. K. Kim, Columbia University Report No. Nevis 149, 1966 (unpublished).
[37] M. Ferro-Luzzi, R. D. Tripp, and M. B. Watson, Phys. Rev. Lett. **8**, 28 (1962).
[38] I. J. General and S. R. Cotanch, Phys. Rev. C **69**, 035202 (2004).
[39] N. V. Shevchenko, A. Gal, and J. Mareš, Phys. Rev. Lett. **98**, 082301 (2007); N. V. Shevchenko, A. Gal, J. Mareš, and J. Révai, Phys. Rev. C **76**, 044004 (2007).
[40] J. K. Kim and F. von Hippel, Phys. Rev. **184**, 1961 (1969).
[41] K. Moriya *et al.* (CLAS Collaboration), Phys. Rev. C **87**, 035206 (2013); R. A. Schumacher and K. Moriya, arXiv:1303.0860 (to be published).
[42] S. M. Flatte, Phys. Lett. B **63**, 224 (1976).
[43] G. Agakishiev *et al.* (HADES Collaboration), arXiv:1208.0205.
[44] J.-J. Xie and B.-C. Liu, Phys. Rev. C **87**, 045210 (2013).